Reducing Greenhouse Effects via Fuel Consumption-Aware Variable Speed Limit (FC-VSL)

Bojin Liu, Dipak Ghosal, *Member, IEEE*, Chen-Nee Chuah, *Senior Member, IEEE*, and H. Michael Zhang

Abstract—Given the heated discussion of climate change and the ever-increasing demand for fossil fuels, the ability to reduce vehicular carbon footprints is of great importance for both environmental and economical reasons. This paper presents a carbon-footprint/fuel-consumption-aware variable-speed limit (FC-VSL) traffic control scheme that targets minimizing the average vehicular fuel consumption on freeways under live traffic conditions. We first formulated the problem of minimizing fuel consumption for a single vehicle under certain traffic conditions as an optimal control problem. By solving the problem, we obtained the optimal vehicular trajectory, which results in minimum fuel consumption. Then, we designed the FC-VSL scheme based on the optimal trajectory. We evaluated the performance of the FC-VSL scheme through detailed simulation. The results show that the FC-VSL scheme can significantly reduce the average fuel consumption and outperform another speed limit scheme that was designed to smooth traffic flow without considering fuel consumption.

Index Terms—Fuel economy, intelligent transportation system, minimize greenhouse gas emissions, optimal control, simulation analysis, variable speed limit, vehicle infrastructure integration, vehicular ad hoc network.

I. INTRODUCTION

THE U.S. Environmental Protection Agency (EPA) ranks the transportation sector, among all end-user sectors, as the second largest contributor to greenhouse gas (GHG) emission [1], which may have profound negative impact on the global climate [2]. Within the transportation sector, vehicles that we drive release more than 1.7 billion tons of CO_2 into the atmosphere each year alone [4]. The vehicular carbon footprint is a measure of the vehicle's environmental impact on climate change in terms of CO_2 emission, which also has a direct relationship with the fuel consumption of vehicles.

As economic growth provides sustaining demands for fossil fuels, the problem of how to reduce vehicular carbon footprint and fuel consumption becomes not only an environmental problem but an economic problem as well. Among all factors that determine the fuel efficiency of an individual vehicle, the impact of speed and acceleration/deceleration is similar among all vehicles.

In this paper, we propose a carbon-footprint/fuel-consumption-aware variable speed limit (FC-VSL) traffic control scheme that targets to reduce average vehicular fuel consumption, and hence carbon footprint, for all vehicles under certain traffic conditions while obeying traffic constraints. This is achieved by first deriving the theoretical optimal movement trajectory that can result in minimum fuel consumption, with the help of an aggregated vehicular instant fuel consumption model. Then, the FC-VSL scheme can be designed, which is designed to regulate vehicles on the road to follow the optimal trajectory as close as possible to achieve fuel consumption that is close to the theoretical optimum. The biggest contribution of this work is that it is the first such traffic control scheme that targets optimal vehicular fuel consumption under live traffic conditions.

We also present a system architecture under which the proposed FC-VSL scheme can be applied. One key component of the system is wireless communication between vehicles and the infrastructure using dedicated short-range communication/wireless access in a vehicular environment (DSRC/WAVE) standards [3]. DSRC/WAVE is a set of emerging standards for vehicle-to-vehicle (V2V) and vehicle-to-infrastructure (V2I) communication. It is part of the Federal Highway Authority's Vehicle Infrastructure Integration initiative, operating in the 5.86–5.92-GHz band allocated by the Federal Communications Commission in the U.S. The proposed FC-VSL scheme employs a combination of DSRC/WAVE-capable vehicles and roadside units (RSUs), a centralized control analysis station, and traditional ITS infrastructure such as loop detectors to form a variable speed limit (VSL) control loop that targets to minimize the overall fuel consumption of all vehicles on the target stretch of the freeway.

The structure of this paper is given as follows: Section II discusses the background of the problem and the related works. Section III provides a description of the problem that we are trying to solve and presents the proposed system architecture. Section IV provides details of how to formulate and solve the problem using optimal control theory. Section V discusses the implementation of the FC-VSL scheme on the simulation platform. Section VI presents the simulation results, and Section VII concludes this paper.

B. Liu and D. Ghosal are with the Department of Computer Science, University of California, Davis, CA 95616 USA (e-mail: frdliu@ucdavis.edu; dghosal@ucdavis.edu).

C.-N. Chuah is with the Department of Electrical and Computer Engineering, University of California, Davis, CA 95616 USA (e-mail: chuah@ucdavis.edu).

M. Zhang is with the Department of Civil and Environmental Engineering, University of California, Davis, CA 95616 USA (e-mail: hmzhang@ucdavis.edu).

II. BACKGROUND AND RELATED WORK

A. Relationship Between GHG Emission, Vehicular Carbon Footprint, Fuel Consumption, and Vehicle Speed

GHG emission, vehicular carbon footprint, and fuel consumption are different but closely related concepts. GHG refers to gases that trap heat in the atmosphere, which may affect the global climate. GHG that enters the atmosphere due to vehicle emissions mainly include carbon dioxide (CO_2) and nitrous oxide (N_2O) (carbon monoxide (CO) is another kind of major vehicular emission gas but is not generally considered to be a GHG) [5]. As CO_2 is the largest contributor of vehicular GHG emission, it is therefore commonly referred to as the vehicular carbon footprint to measure a vehicle's emission's impact on climate change [6]. Since CO_2 is generated through the burning of fossil fuels, vehicular carbon footprint has an almost linear relationship with the fuel consumption [7]. Therefore, techniques for improving the fuel efficiency for vehicles cannot only result in less demand for fossil fuels, which provides economic incentives, but can also reduce the carbon footprint of vehicles, which can have positive environmental implications as well. In this paper, for ease of discussion, we interchangeably use carbon footprint and fuel consumption due to the linear relationship between the two.

B. Vehicular Carbon Footprint and Fuel Consumption

Although individual vehicle's exact fuel consumption signature could significantly vary for different models, it is well studied that high vehicle speed and dramatic acceleration/deceleration can result in low fuel efficiency. In [8], it is shown that speed limit control is the most cost effective approach for curbing vehicle carbon emissions. It is observed that a stronger enforcing of 70-mi/h speed limit would cut carbon emissions by nearly 1 million tons of carbon per annum. A 60-mi/h limit would nearly double this reduction [8]. Other more sophisticated speed limit control schemes have been proposed to smooth vehicular traffic [12], which may also be able to reduce the average vehicular carbon footprint. However, none of these approaches were designed toward the goal of carbon footprint minimization, and the increased fuel efficiency can only be considered as a side benefit.

C. Fuel Consumption Models

In this paper, we present a speed control scheme that is built toward the goal of minimizing overall vehicular fuel consumption under certain traffic conditions. To accurately estimate/measure the fuel consumption, we need an accurate fuel consumption model that defines the instant quantitative relationship between fuel consumption and physical properties of the traveling vehicle, such as speed and acceleration/deceleration rate, etc. There are many models/software providing fuel consumption/emission modeling. MOBILE6 and MOVES [13], [14] are computer programs provided by the U.S. EPA for average emission models for highway vehicles. Except for MOVES2010, they are not suitable for our purpose since they are all average estimation models and cannot be used for estimation within an hour, whereas we need a model that provides instantaneous

estimation of fuel consumption based on speed and acceleration rate. MOVES2010 is the latest version of the MOVES family. It can support fuel consumption estimation at a finer time frame. The EMission FACtors (EMFAC) model [15] is a software model provided by the California Air Resource Board that can be used to estimate emissions. Despite its capability, neither MOVES2010 nor EMFAC are suitable for our project since it is hard for us to extract analytical relationships between the vehicle's state and the corresponding instant fuel consumption rate from the software. The U.K. National Atmospherics Emissions Inventory (NAEI) Emission Factor Database [16] provides quantitative relationship between vehicle speed and acceleration rate to emissions. However, it is also an average model that would not be accurate enough for our purpose of instantaneous emission estimation. The model presented in [7] at the Conference of Australian Institutes of Transportation Research (CAITR) is a model based on which a proprietary fuel consumption/emission modeling software was built. It is an instantaneous model that models an exact relationship between vehicle physical properties to fuel consumption and emissions at every instant of time. We adopt CAITR as the fuel consumption model in our study.

D. Variable Speed Limit (VSL)

VSLs are speed limits that change based on road, traffic, and weather conditions [9]. VSL systems have been around for about 40 years [10]. Most of the VSL systems implemented right now are designed to potentially reduce driver error and speeds and to enhance the safety of roadways. For example, there has been an experimental practice in Arizona where a fuzzy control system is designed to determine the speed limit based on a category of conditions such as road surface condition, wind speed, and visibility [11]. Another experimental VSL system in Colorado was designed to identify vehicle-specific safe operating speeds for long downgrades. The system computes a safe speed based on the vehicle weight, speed, and axle configuration. The calculated speed limit is displayed via a variable message sign (VMS) [11]. There are also many other practical VSL systems deployed in the U.S. and around the world that can be found in [11]. In [17], the authors proposed a VSL scheme for freeway workzones that targets to improve traffic flow throughput and accident minimization.

E. Fuel-Consumption-Aware Vehicle Control Techniques

There have been previous studies on vehicle control for the purpose of reducing fuel consumption for individual vehicles. In particular, in the research of hybrid electric vehicles, techniques such as dynamic programming and optimal control have been utilized to derive near-optimal power management strategies, in which the sequence of control actions, such as gear shifting, and power splitting between the combustion engine and the electric engine are selected to achieve near-optimal fuel consumption [26], [27]. In the area of adaptive cruise control [28] and autonomous intelligent cruise control [29], there have also been works focusing on increasing fuel efficiency. In [30], an intelligent fuzzy cruise controller was designed and fully implemented to minimize fuel cost while addressing the
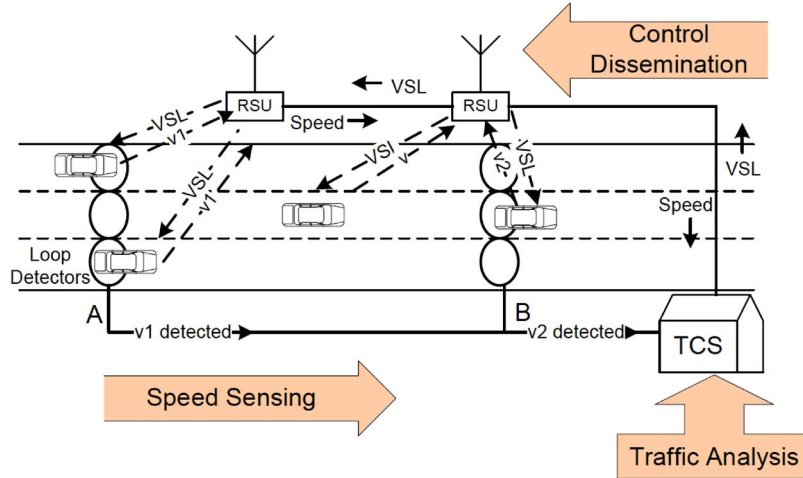
Fig. 1. System architecture for implementing FC-VSL.

driver's driving need. In [31], a fuel-optimal cruise controller is designed for heavy trucks, taking into consideration Global Positioning System and road topographical information. Another field that is more related to our work is to use V2V and V2I communication to design vehicle control schemes for higher fuel efficiency. For instance, in [32], V2I communication is utilized to transmit traffic signal control information to vehicles, so that vehicle engines could be shut off to avoid wasting fuel while waiting at signals. All of the aforementioned works differ from our work in the sense that they are designed to reduce individual vehicle's fuel consumption, considering only individual vehicles' running state. On the other hand, the speed control scheme proposed in this work is a system-level traffic control scheme that targets to minimize the total fuel consumption of all vehicles for a specific section of road, under live system-level traffic conditions.

III. GOALS AND PROPOSED ARCHITECTURE

A. Problem Description and Design Goals

The purpose of this project is to design FC-VSL control under certain live traffic conditions. Traffic conditions on the freeway may change due to different factors. Consider an example of a lane drop scenario where several lanes are blocked due to either a construction zone or accident. Under certain traffic density, the average free flow speed at the lane drop location may be significantly reduced. Vehicles upstream of the lane drop location need to prepare for slowdown. Some speed limit control schemes were proposed for this kind of scenario to reduce the possible shock wave and traffic jitter created by the lane drop [17]. However, in our project, we proposed a VSL scheme that targets to minimize the overall fuel consumption of all vehicles. By formulating the problem as an optimal control problem, we first derive the optimal trajectory for an individual vehicle that results in minimum fuel consumption. Then, we designed the VSL in order for the traffic to follow the optimal trajectory as close as possible so that the overall fuel consumption could be reduced toward the minimum. Our solution to this case study could be generalized to include all

scenarios where average traffic speeds have changed at different locations of the freeway.

B. Architecture Overview

Fig. 1 shows the architecture of the proposed system and an example scenario where there is a speed drop from average speed of $v1$ to $v2$ on a stretch of freeway. We consider a centralized speed control system with three key components: 1) speed sensing; 2) traffic analysis; and 3) control dissemination. The speed sensing components are mainly responsible for sensing and collecting the average speed of vehicles at different locations of the freeway. As indicated in the figure, we could employ traditional techniques such as loop detectors [18] for speed sensing, or we could employ the vehicle's onboard sensor for speed sensing and transmit the vehicle's speed and locations to RSUs through DSRC/WAVE. RSUs will be deployed along the freeway and directly connected to the traffic control station (TCS). The TCS is the place where traffic analysis is performed. At the TCS, upon receiving live vehicle speed information at different locations, the vehicle trajectory that can result in minimum fuel consumption for this stretch of road will be calculated. The trajectory is calculated as a system optimal trajectory in the sense that, if every vehicle closely follows the trajectory, the overall fuel consumption of all vehicles will be reduced to minimum. At last, the calculated optimal trajectory will be transmitted from the RSU back to the vehicles through the DSRC/WAVE channel and serve as the VSL control signal. Upon receiving the VSL signal, the vehicle's onboard processing unit will automatically calculate the speed limit corresponding to its current location. The vehicle will then comply with the new speed limit. We can envision scenarios (e.g., automated cruise control) where the speed limit can be automatically applied by the vehicle, or an alert message will be sent to the driver to adjust the speed accordingly. How the users/drivers react to the speed limit is out of the scope of this paper. We focus on predicting the potential theoretical fuel consumption savings, assuming the best case scenario where the vehicle or rational driver can adjust the speed according to the optimal trajectory as close as possible.

IV. MINIMUM FUEL CONSUMPTION UNDER LIVE TRAFFIC CONDITION FOR A SINGLE VEHICLE

A. Problem Formulation

Considering, at time $t_0 = 0$, a vehicle on the freeway at location s_0 traveling at the speed of v_0. At location s_1 ($s_1 > s_0$), there is a traffic condition that causes the vehicle's speed to reduce to v_1. Examples of such conditions include but are not limited to reduced road capacity due to drop of lanes, sharp turns, severe weather conditions (e.g., flooded/icy road), bridges, and toll booth. We need to find an optimal trajectory that can minimize the fuel consumption for this vehicle traveling between s_0 and s_1.

1) System Model: For a single vehicle, state vector $\mathbf{x}(t)$ is defined as

$$\mathbf{x}(t) \triangleq [x_1(t) \; x_2(t)]^T = [s(t) \; v(t)]^T \tag{1}$$

where $s(t)$ is the distance from s_0, and $v(t)$ is the speed of the vehicle. The control vector only contains the acceleration rate

$$\mathbf{u}(t) \triangleq [a(t)]^T. \tag{2}$$

The ordinary differential equation that defines the system dynamic is

$$\dot{\mathbf{x}}(t) = \begin{bmatrix} \dot{x}_1(t) = v(t) \\ \dot{x}_2(t) = a(t) \end{bmatrix}. \tag{3}$$

2) Optimal Control Problem Formulation: We formulate the problem as an optimal control problem as follows: find an optimal control $a^*(t)$ and corresponding trajectory $x^*(t)$ so that the performance measure

$$\boldsymbol{J} = \int_{t_0}^{t_f} c\left(\mathbf{x}(t), \mathbf{u}(t), t\right) dt \tag{4}$$

is minimized, where $c(\mathbf{x}(t), \mathbf{u}(t), t)$ is the instantaneous fuel consumption model [7], which is given by

$$c = \begin{cases} \alpha, & \text{if } a \le -\frac{R_a(t) + R_r(t)}{M_v} \\ \alpha + \beta_1 R_T(t) v(t), & \text{if } a \in \left(-\frac{R_a(t) + R_r(t)}{M_v}, 0\right) \\ \alpha + \beta_1 R_T(t) v(t) \\ \quad + \frac{\beta_2 M_v a(t)^2 v(t)}{1000}, & a \ge 0 \end{cases} \tag{5}$$

where $R_T(t)$, $R_a(t)$, and $R_r(t)$ are the tractive force, air drag force, and rolling resistance, respectively. They are dynamically calculated as follows [19]:

$$R_T(t) = M_v a(t) + R_a(t) + R_r(t) + R_a(t) + R_g(t) \tag{6}$$
$$R_a(t) = \frac{\rho}{2} C_D A_f v^2(t) \tag{7}$$
$$R_r(t) = 0.01 \frac{1 + v(t)}{44.73} M_v g. \tag{8}$$

The definitions and values of the parameters from (5)–(8) are defined in Table I. Note that the default values of the parameters of the fuel consumption model assumes that the vehicle travels on a flat surface (i.e., grade force $R_g(t) = 0$), under standard

TABLE I
PARAMETER DEFINITIONS AND VALUES

Parameter	Definition	Value
α	Idle fuel consumption rate	$0.375 mL/s$
β_1	Efficiency parameter	$0.09 mL/kJ$
β_2	Energy-acceleration efficiency parameter	$0.03 mL/(kJ.m/s^2)$
M_v	Average vehicle mass	$1400 kg$
ρ	Air density	$1.2256 kg/m^3$
C_D	Drag coefficient	0.54
A_f	Average vehicle frontal area	$2.1 m^2$
g	Standard gravity	$9.8 m/s^2$

air pressure and that there is no wind. However, the fuel consumption model can easily be adapted to other scenarios that can reflect a real environment with different wind speeds, grade levels, etc. This is achieved by adjusting the values of the parameters of R_T.

We define the Hamiltonian as follows:

$$\mathcal{H}\left(\mathbf{x}(t), \mathbf{f}(t), \mathbf{p}(t)\right) = \mathbf{f}(t) \cdot \mathbf{p}(t) + c(t) \tag{9}$$

where $c(t) = c(\mathbf{x}(t), \mathbf{u}(t), t)$, $\mathbf{f}(t) = \begin{bmatrix} \dot{x}_1(t) = v(t) \\ \dot{x}_2(t) = a(t) \end{bmatrix}$, and $\mathbf{p}(t) = \begin{bmatrix} p_1(t) \\ p_2(t) \end{bmatrix}$ is defined as the costates of $\mathbf{x}(t)$. $\mathbf{f}(t)$ describes how the dynamic system evolves over time. Both $\mathbf{f}(t)$ and $\mathbf{p}(t)$ are in vector form.

From the Pontryagin maximum principle, in terms of the Hamiltonian, the first-order optimality conditions for $\mathbf{u}^*$ to be an optimal control are

$$\dot{\mathbf{x}}^*(t) = \frac{\partial \mathcal{H}}{\partial \mathbf{p}}\left(\mathbf{x}^*(t), \mathbf{u}^*(t), \mathbf{p}^*(t)\right)$$
$$\Rightarrow \begin{cases} \dot{s}^*(t) = \mathcal{H}_{p_1} = v^*(t) \\ \dot{v}^*(t) = \mathcal{H}_{p_2} = a^*(t) \end{cases} \tag{10}$$

$$\dot{\mathbf{p}}^*(t) = -\frac{\partial \mathcal{H}}{\partial \mathbf{x}}\left(\mathbf{x}^*(t), \mathbf{u}^*(t), \mathbf{p}^*(t)\right)$$
$$\Rightarrow \begin{cases} \dot{p_1}^*(t) = \mathcal{H}_{x_1} = 0 \\ \dot{v}^*(t) = \mathcal{H}_{x_2} = -\mathcal{H}_v \end{cases} \tag{11}$$

$$\frac{\partial \mathcal{H}}{\partial \mathbf{u}}\left(\mathbf{x}^*(t), \mathbf{u}^*(t), \mathbf{p}^*(t)\right) = 0 \tag{12}$$

$$\mathcal{H}\left(\mathbf{x}^*(t), \mathbf{u}^*(t), \mathbf{p}^*(t)\right) = 0 \tag{13}$$

and (10)–(12) must be true for all $t \in [t_0, t_f]$. Since we are modeling a midsize vehicle on the freeway, the optimal trajectory and optimal control should also be under the constraints of maximum and minimum speed limits on freeways, i.e.,

$$v(t) \in [v_{\min}, v_{\max}], \qquad t \in [t_0, t_f]. \tag{14}$$

The default values of $v_{\min}$ and $v_{\max}$ were set to 17 and 25 m/s, respectively. Note that the $\mathbf{f}(t)$ in Hamiltonian in (10)–(13) have been substituted according to definition and (2).

3) Approximation for the Fuel Consumption Model: Notice that the instant fuel consumption by (5) is a noncontinuous piecewise function with respect to acceleration rate **a**. The discontinuity happens at two places when $a = 0$ and $a = \Phi = -R_a(t) + R_r(t)/M_v$. In order for us to find the optimal solution, we need to smooth (5) so that the instant fuel consumption equation is guaranteed to have first derivative at all acceleration
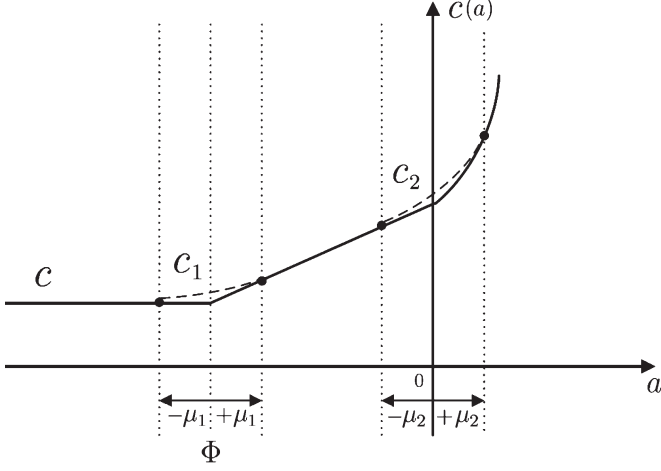
Fig. 2. Approximation of the fuel consumption model with respect to acceleration rate. The solid line represents the original function defined by (5), and the two dotted curves are the two quadratic approximation functions defined in (15) and (16).

rates. We achieve this by using two quadratic functions to approximate the original function at the two turning points. Fig. 2 shows how we achieve the approximation. In general, at each turning point, we seek a quadratic function so that the following hold: 1) It intercepts with (5) at two points (below and above the corner point); 2) both points are of equal distance μ to the corner point; and 3) the quadratic function's derivatives at the two intercepting points are equal to (5)'s first declivities at the corresponding points. Specifically, we define two approximation quadratic functions as follows:

$$c_1(a) = A_1 a^2 + B_1 a + C_1, \qquad a \in [\Phi - \mu_1, \Phi + \mu_1] \quad (15)$$

$$c_2(a) = A_2 a^2 + B_2 a + C_2, \qquad a \in [-\mu_2, \Phi + \mu_2]. \quad (16)$$

For c_1, we have

$$
\begin{cases}
\dot{c}_1(\Phi - \mu_1) = \dot{c}(\Phi - \mu_1) \\
\quad \Rightarrow 2A_1(\Phi - \mu_1) + B_1 = 0 \\
\dot{c}_1(\Phi + \mu_1) = \dot{c}(\Phi + \mu_1) \\
\quad \Rightarrow 2A_1(\Phi + \mu_1) + B_1 = \frac{\beta_1 M_v v}{1000} \\
c_1(\Phi - \mu_1) = c(\Phi - \mu_1) \\
\quad \Rightarrow A_1(\Phi - \mu_1)^2 + B_1(\Phi - \mu_1) + C_1 = \alpha.
\end{cases}
\quad (17)
$$

Then, we can solve (17) for A_1, B_1, and C_1, i.e.,

$$
\begin{cases}
A_1 = \frac{\beta_1 M_v v}{4000 \mu_1} \\
B_1 = \frac{\beta_1 M_v v(\mu_1 - \Phi)}{2000 \mu_1} \\
C_1 = \alpha + \frac{B_1^2}{4A_1}.
\end{cases}
\quad (18)
$$

Similarly, for c_2, we have

$$
\begin{cases}
\dot{c}_2(-\mu_2) = \dot{c}(-\mu_2) \\
\quad \Rightarrow 2A_2(-\mu_2) + B_2 = \frac{\beta_1 M_v v}{1000} \\
\dot{c}_2(\mu_2) = \dot{c}(\mu_2) \\
\quad \Rightarrow 2A_2(\mu_2) + B_2 = \frac{\left(\beta_1 + 2\frac{\beta_2}{1000}\mu_2\right)(M_v v)}{1000} \\
c_2(-\mu_2) = c(-\mu_2) \\
\quad \Rightarrow A_2(-\mu_2)^2 + B_2(-\mu_2) + C_1 = \frac{\beta_1 R_t v \mu_2}{1000} + \alpha
\end{cases}
\quad (19)
$$

and the solution to (19) is

$$
\begin{cases}
A_2 = \frac{\beta_2 M_v v}{2000} \\
B_2 = \frac{\beta_2 M_v v \mu_2}{1000} \\
C_2 = A_2 \mu_2^2 + \frac{\beta_1 R_t v \mu_2}{1000} + \alpha.
\end{cases}
\quad (20)
$$

When μ_1 and μ_2 are significantly small (they were both set to 0.00001 m/s^2), we can use the following smooth piecewise function, with respect to acceleration rate **a**, to approximate (5):

$$
c_{\text{approx}} =
\begin{cases}
\alpha, & a \in [a_{\min}, \Phi - \mu_1) \\
c_1, & a \in [\Phi - \mu_1, \Phi + \mu_1] \\
\alpha + \beta_1 R_T(t)v(t), & a \in (\Phi + \mu_1, -\mu_2) \\
c_2, & a \in [-\mu_2, \mu_2] \\
\alpha + \beta_1 R_T(t)v(t) \\
\quad + \frac{\beta_2 M_v a(t)^2 v(t)}{1000}, & a \in (\mu_2, a_{\max}].
\end{cases}
\quad (21)
$$

B. Optimal Control Solution

1) Methodology: Ideally, using the indirect method for solving the optimal control problem, from (12), we can solve $\mathbf{a}^*(t)$ in terms of $\mathbf{x}^*(t)$ and $\mathbf{p}^*(t)$ and then substitute $\mathbf{a}^*$ in (10) and (11). Then, we can solve the boundary value problem formed by (10) and (11). However, since the Hamiltonian $\mathcal{H}$ is a piecewise function, it is extremely difficult to find analytical solutions using the indirect method as described. Instead, the numerical Gauss pseudospectral method (GPM) is used to obtain the solution. The GPM is an orthogonal collocation method where the collocation points are the Legendre–Guass (LG) points [20]. By using the GPM, the first-order optimality condition specified by (12) could be transcribed into a nonlinear program (NLP). This is achieved by using Lagrange polynomials to approximate both the state and costate of the system. Specifically, with the initial state and states values at the N LG points, a Lagrange polynomial is used to approximate the state. On the other hand, with the final value of the costate and costate values at the N LG points, another Lagrange polynomial is used to approximate the costate. Specifically, for our problem, the state is approximated as follows:

$$\mathbf{x}(t) \approx \mathbf{X}(t) = \sum_{i=0}^{N} \mathbf{X}(t_i) L_i(t) \quad (22)$$

where $L_i(t)(i = 0, \ldots, N)$ are defined as

$$L_i(t) = \prod_{j=0, j \neq i}^{N} \frac{t - t_j}{t_i - t_j}. \quad (23)$$

Similarly, the control is approximated as follows:

$$\mathbf{u}(t) \approx \mathbf{U}(t) = \sum_{i=1}^{N} \mathbf{X}(t_i) L_i^*(t) \quad (24)$$

where

$$L_i^*(t) = \prod_{j=1, j \neq i}^{N} \frac{t - t_j}{t_i - t_j} \quad (25)$$

and the costates

$$\mathbf{p}(t) \approx \mathbf{P}(t) = \sum_{i=1}^{N+1} \mathbf{P}(t_i) L_i^c(t) \qquad (26)$$

where

$$L_i^c(t) = \prod_{j=1, j \neq i}^{N+1} \frac{t - t_j}{t_i - t_j}. \qquad (27)$$

After the approximation, the first-order optimality condition, as defined in (12), could be discretized into a nonlinear system of equations with the following form:

$$\begin{cases} \sum_{i=0}^{N} \mathbf{X}_i D_{ki} = \mathbf{f}_k \\ \sum_{i=1}^{N} \mathbf{P}_i D_{ki}^c + \mathbf{P}_f D_{kN+1}^c = -\frac{\partial c_k}{\partial \mathbf{X}_k} - \mathbf{P}_k^T \frac{\partial \mathbf{f}_k}{\partial \mathbf{X}_k} \\ \frac{\partial c_k}{\partial \mathbf{U}_k} + \mathbf{P}_k^T \frac{\partial \mathbf{f}_k}{\partial \mathbf{U}_k} = 0 \\ c_k + \mathbf{P}_k^T \mathbf{f}_k = 0 \end{cases} \qquad (28)$$

where $D_{ki} = \dot{L}_i(t_k) = \sum_{i=0}^{N} (\prod_{j=0, j \neq i}^{N} (t_k - t_j) / \prod_{j=0, j \neq i}^{N} (t_i - t_j))$, $\mathbf{X}_i \equiv \mathbf{X}(t_i)$, $\mathbf{P}_i \equiv \mathbf{P}(t_i)$, $\mathbf{U}_i \equiv \mathbf{U}(t_i)$, and $c_i \equiv c(t_i)$. Numerically solving (28) would generate the solution for the optimal control problem.

Another approach to solve the optimal control problem is the direct method. The direct method discretizes the optimal control problem by discretizing the system dynamics, constraints, and cost objective functions using (22), (24), and (26), in a fashion similar as previously described, and thus transcribes the optimal control problem into an NLP problem. It can be shown that the discretized optimality condition by (28) from the indirect method corresponds to the Karush–Kuhn–Tucker conditions of the NLP problem transcribed in the direct method [20].

We employ General Pseudospectral OPtimal Control Software (GPOPS) [22] to obtain the optimal control solution. GPOPS is a numerical package for solving the optimal control problem that implements the GPM. It automatically transcribes the optimal control problem into the corresponding NLP problem and then uses an NLP solver to solve for the numerical solution. The default NLP solver employed by GOPOS is SNOPT [23].

2) Optimal Solution for a Sample Scenario: In a sample scenario where $s_0 = 0$, $s_1 = 600$ m, $v_0 = 25$ m/s, $v_1 = 20$ m/s, and $v_{\min} = 17$ m/s, the solution of the optimal control problem defined in the previous section can be found in Figs. 3 and 4. The initial guess of the control provided to GPOPS is set to $a(t) = -0.1875$ m/s^2 for all $t \in [t_0, t_f]$. This is a naive control scheme in which the vehicle's speed is constantly decreased to the target speed. The tolerance of the cost objective was set to 0.0001 ml, and number of LG nodes was set to 50 as default.

Fig. 3 shows the optimal trajectory of the vehicle's speed. It shows that, to achieve minimum fuel consumption, the vehicle first needs to decrease its speed below the target speed to around 18.6 m/s at around 17 s and then gradually increase its speed to the target speed of 20 m/s. This is a bit counterintuitive at first since it is generally believed that an acceleration phase would have consumed more fuel than a pure deceleration process. However, a closer examination of the fuel consumption model
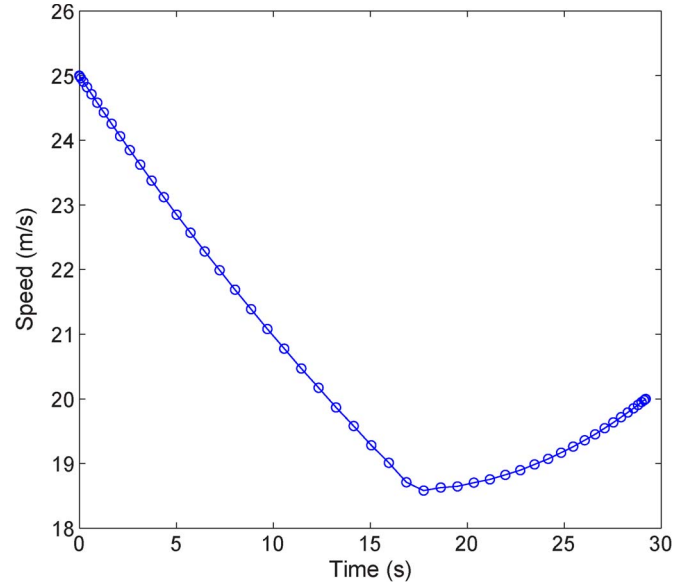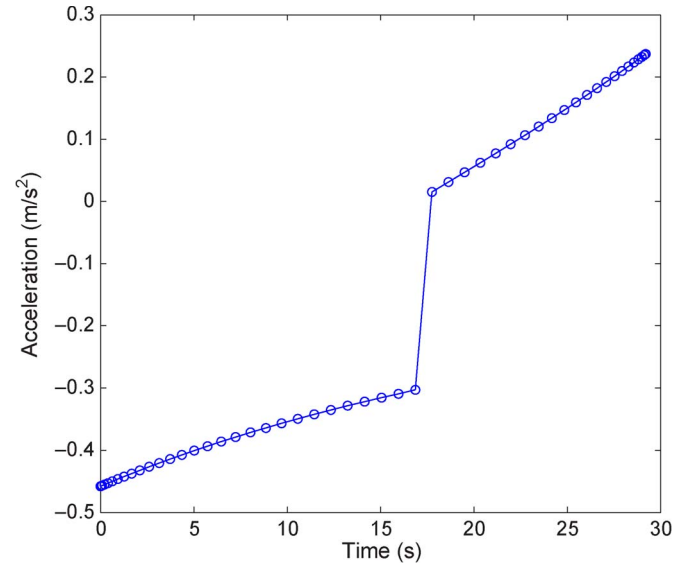

Fig. 3.   Optimal speed trajectory.

Fig. 4.   Optimal control (acceleration) trajectory.

of (5) reveals that, when $a \geq 0$, although the acceleration rate $a(t)$ has a high impact on the total fuel consumption in the third term, vehicle speed $v(t)$ mandates both the second and third terms. The implication is that, at lower speed, the impact of high acceleration rate on the fuel consumption could be offset by the impact of the lower speed. Another thing to notice is that, although, in the optimal trajectory, there are periods when the speed is lower than the target speed, the overall traveling time for the optimal trajectory (about 29.27 s) is even less than the time it takes if the vehicle travels the entire stretch of road at the target speed (travel time = 30 s = 600 m/20 m/s). In addition, the speed limit constraint defined in (14) is obeyed for the optimal trajectory. Fig. 4 shows the optimal control (the optimal acceleration) trajectory. The switching point from deceleration to acceleration corresponds to the time shown in Fig. 3.

Fig. 5 shows the convergence of the cost objective through iterations as the transcribed NLP problem is solved. In addition, from Fig. 4, it may seem that the transition around 17 s may
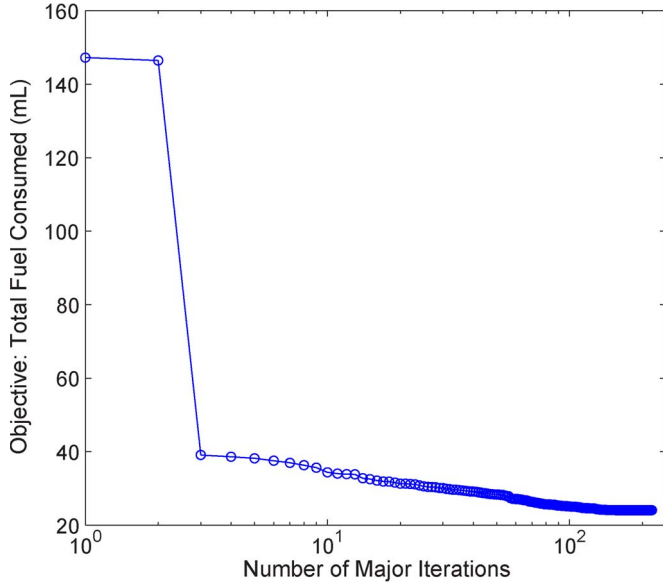
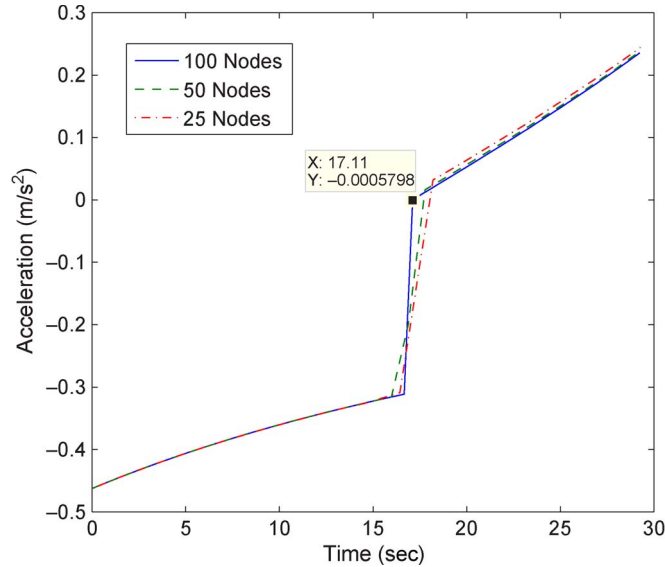Fig. 5. Convergence of cost objective.

Fig. 6. As the number of LG node increases, the control converges to optimal trajectory.

not be instantaneous. It is important to determine whether an instantaneous switch exists, as the optimal control obtained will be used to develop fine-grained VSL control schemes. Fig. 6 shows the optimal controls obtained from GPOPS with different numbers of LG nodes. As the number of LG nodes increases, the results obtained from GPOPS approaches the theoretical optimal control. We can see the trend of having an instantaneous switch from deceleration to acceleration around 17 s.

3) Sensitivity Analysis: The previous section shows the optimal trajectory for a particular scenario with the initial and terminating speeds (v_0 and v_1) set to 25 and 20 m/s and the control distance (s_1) set to 600 m. This section examines how the optimal trajectory would change with respect to different values of those parameters.

Fig. 7 shows different optimal trajectories with the same initial and control distance but different terminating speeds. We can see that, in all cases, the trajectory contains a decel-
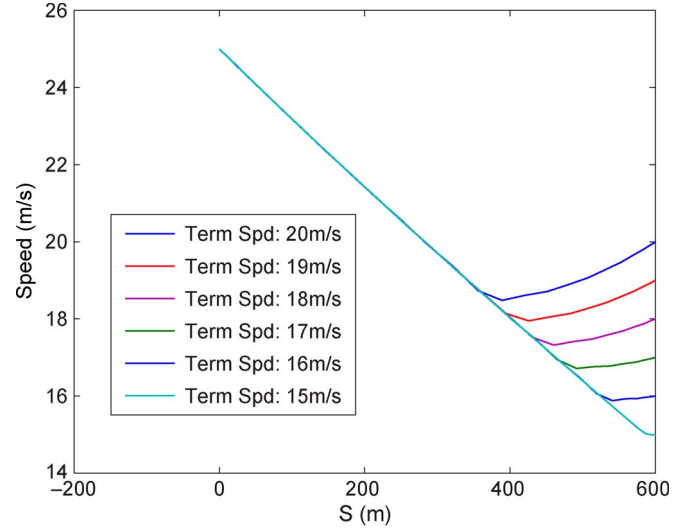
Fig. 7. Optimal trajectories with different terminating speeds (v_1) and the same initial speed ($v_0 = 25$ m/s) and control distance ($s_1 = 600$ m).

eration phase with a similar deceleration rate at the beginning. After the deceleration phase comes the acceleration phase, in which different trajectories slowly reach their target terminating speeds. The reason that all trajectories share the same deceleration phase is that, given $\mathbf{a}(t)$ at the deceleration phase, the engine provides no tractive force (i.e., $R_T \leq 0$, or $\mathbf{a}(t) \leq -R_a(t) + R_r(t)/M_v$), and according to the fuel consumption model specified by (5), the vehicle will only consume the fuel at the idle fuel consumption rate (α). The idle fuel consumption rate is significantly smaller than the other rates specified in (5). Therefore, to achieve minimum fuel consumption, the vehicle needs to operate at the idle fuel consumption rate as long as possible, thus the initial deceleration phase. However, as the vehicle needs to achieve a certain terminating speed, it will need to start a slow acceleration phase at some point. The higher the terminating speed, the sooner the acceleration phase needs to start, because the vehicle needs to maintain a relatively small average acceleration rate in order not to consume too much fuel in the acceleration phase.

Fig. 8 shows different optimal trajectories with the same initial and terminating speed but different control distances (s_1). Fig. 8(a) shows the results for shorter s_1. As we can see, there are two types of trajectories in Fig. 8(a), i.e., decelerate–accelerate trajectories (D-A trajectories) similar to those in Fig. 7 at larger s_1 ($s_1 \geq 300$ m) and decelerate–decelerate trajectories (D-D trajectories), where the vehicle travels at the idle fuel consumption rate at first and then decelerates straight to its target terminating speed. For the D-A trajectories, due to similar reasons presented in the aforementioned section, the vehicle needs to travel at the idle fuel consumption rate as long as possible and then slowly accelerates to its target terminating speed. The shorter the s_1 is, the shorter the deceleration phase has to be so that there will be enough distance left for the gentle acceleration phase to reach the target terminating speed. For the D-D trajectories, their s_1 are too short so that there would not be enough distance for the vehicle to reduce its speed to the terminating speed if the vehicle only travels at the idle fuel consumption rate. Therefore, a second "harder" deceleration phase is needed for D-D trajectories.
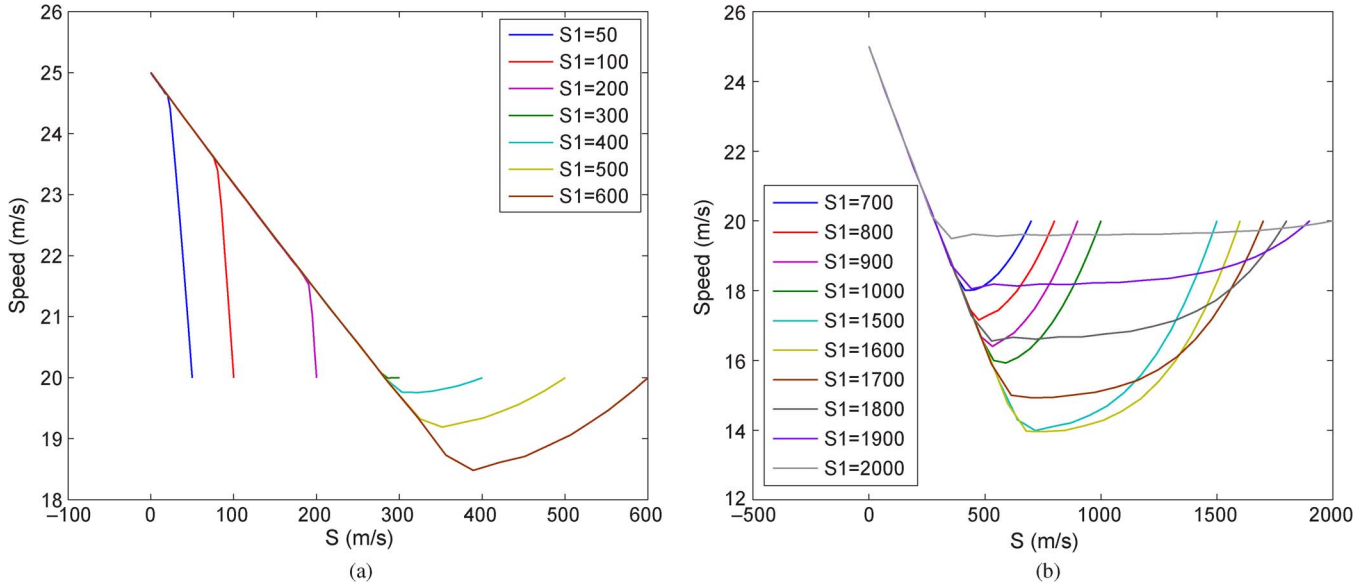
Fig. 8. Optimal trajectories with different control distances (s_1), and the same initial and terminating speeds $(v_0 = 25 \text{ m/s}, v_1 = 20 \text{ m/s})$. (a) Optimal trajectories with small s_1. (b) Optimal trajectories with large s_1.

Fig. 8(b) shows the results for larger s_1. It also contains two types of trajectories: 1) the D-A trajectories as described in the preceding section at smaller s_1 $(s_1 \leq 1700 \text{ m})$ and 2) the decelerate–slow-acceleration trajectories (D-sA trajectories) at larger s_1. For the D-sA trajectories, as s_1 increases, the deceleration phase becomes shorter, instead of getting larger as D-A trajectories do. As a result, the acceleration phase of the D-sA trajectories has higher average speed but lower average acceleration rate than D-A trajectories. The reason for this change of trajectory types is because, for D-A trajectories, as s_1 increases, the deceleration phase cannot indefinitely increase since, if s_1 becomes too large, the acceleration phase would become much longer, and the fuel saved at the deceleration phase may not be enough to offset the fuel consumption generated in the acceleration phase. Therefore, a more gentle acceleration phase with smaller average acceleration is required for a large s_1.

V. VARIABLE SPEED LIMIT CONTROL WITH OPTIMAL FUEL CONSUMPTION

The solution to the formulated optimal control problem provides theoretical minimum fuel consumption for a single vehicle under certain traffic conditions. Using the optimal trajectory as a guideline, a VSL control scheme could be designed and applied to all vehicles on the street, so that the aggregated fuel consumption of all vehicles could be reduced. This approach differs from other VSL schemes in the sense that it is built toward the goal of minimizing aggregated fuel consumptions of all vehicles, whereas most other VSL schemes are targeting smoothing traffic flows and increasing safety. This section discusses the details of the design of the FC-VSL.

A. FC-VSL

Suppose that a traffic condition similar to the scenario described in the previous sections (average speed drop within a certain distance) is observed by the ITS system. The optimal trajectory for all vehicles to follow is then calculated at the TCS based on the average initial and terminating speed (v_0 and v_1) and the control distance (s_1). The speed values in the optimal trajectory at different locations will be used to set the speed limits for all vehicles at corresponding locations. The VSL control signal, in the form of a sequence of speed limit/location pairs for the target stretch of the road, will be broadcasted to all vehicles through DSRC/WAVE communication. (For coarse-grained VSL control, traditional VMSs could also be used.) Upon receiving the VSL control signals, each vehicle will set its speed limit according to its current location and corresponding optimal speed limit. According to the mobility model, each vehicle will keep increasing its speed until it either reaches the speed limit or is blocked by another vehicle in front of it. Ideally, when each vehicle exactly follows the optimal trajectory by always traveling at the speed limit, it can result in minimum fuel consumption, thus achieving global minimum fuel consumption for the target stretch of the freeway.

However, we would expect the actual global fuel consumption to be suboptimal for live traffic, because not all vehicles are able to always travel at the speed limit and follow the optimal trajectory. First, vehicles on the road travel under the constraints of the current traffic flow condition, in which they may be blocked by other vehicles. Second, the speed limit controls applied are only the upper limits of the vehicle speed, and drivers may randomly opt to travel at a lower speed some of the time. Third, the optimal trajectory is continuous, whereas the speed limit control applied to the vehicle is discrete, no matter how fine the control granularity is. We evaluate the performance of the proposed VSL scheme under these constraints through detailed simulation in the succeeding sections. Our results show that, under the aforementioned constraints, although the average fuel consumption under the proposed VSL scheme is suboptimal, it still achieves much lower fuel consumption than either no-control or another simple VSL approach. The impacts

of the constraints on the performance of the proposed VSL are also examined.

VI. Evaluation of Optimal Carbon Footprint Aware Variable Speed Limit Using VGSim

We used VGSim [21] to evaluate the performance of the proposed VSL scheme. VGSim is an integrated networking and microscopic vehicular mobility simulation platform. It adopts a finer resolution Nagel-Schreckenburg (N-S) [24] vehicle mobility model and employs Jist/SWANS [25] for wireless network simulation. The N-S model is a car-following cellula automata (CA) mobility model, in which both time and space are discrete. Specifically, in the modified N-S model employed by VGSim, the update time interval and cell size are 0.1 s and 0.1 m, respectively [33]. VGSim also implements a closed-loop integration of the mobility model and wireless communication simulation module. The ability to simulate V2I wireless communication with the fine-grained realistic mobility model enables us to examine the proposed FC-VSL scheme under a fine-grained control time frame.

We extended VGSim with the ability to record vehicle fuel consumption. At each time step, the fuel consumed in that time step is calculated based on the current speed and acceleration of the vehicle, according to the instant fuel consumption model defined in (5). The fuel consumption per time units is recorded during the simulation and used later to calculate the total fuel consumption for a vehicle.

For each vehicle, at every control time step, the vehicle determines its current speed according to the vehicle's current location. Specifically, it calculates its current speed limit by interpolating between two closest data points in the optimal trajectory. If the vehicle's current speed is larger than the calculated speed limit, the vehicle will reduce its speed to the new speed limit. The fuel consumption for each vehicle at each time step is recorded, and the total fuel consumption is calculated when the vehicle travels out of the freeway.

A. Limitation of Using the CA Model

One challenging issue encountered in implementing the FC-VSL in VGSim is that VGSim adopts the CA model for vehicular mobility; therefore, it cannot model arbitrary real values of the speed. This implies that, for instance, although the optimal trajectory may indicate a deceleration from 24.9 to 24.0 m/s, the actual value of speed limit set by VGSim will remain 24 m/s. This will not result in a deceleration of the vehicle and thus may incur more fuel consumption. A similar situation could also happen in the acceleration phase. Thus, one would expect that the instant fuel consumption with respect to time produced by VGSim will form a zig-zag pattern around the optimal instant fuel consumption curve. Fig. 9 shows such an example. The results are produced under the same example scenario, as described in the preceding optimal control section. The line with data points as circles shows the optimal instant fuel consumption with respect to time. The line with data points as stars shows the results produced by VGSim. As discussed in the optimal control section, the switching point from deceleration to acceleration happens around time 17 s. In
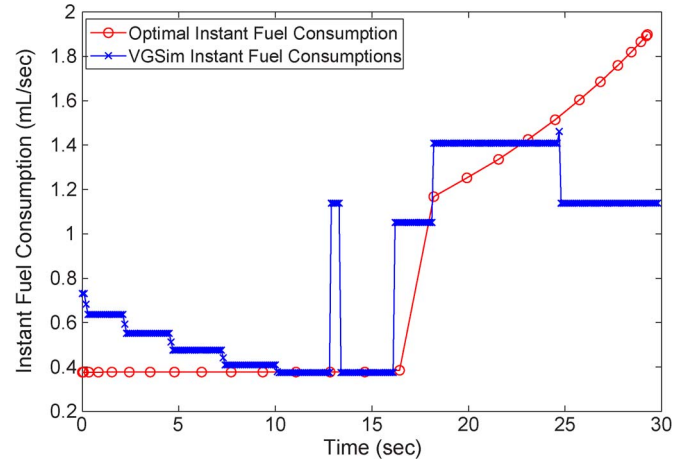

Fig. 9. Comparison of instant fuel consumption trajectory between theoretical optimal control and carbon-aware VSL control using VGSim.

general, VGSim tends to overestimate fuel consumption at the deceleration phase and underestimate at the acceleration phase. Since the example scenario is a deceleration process as a whole, VGSim tends to overestimate the fuel consumed. However, in general, as shown in the figure, VGSim can produce results following the trend of the optimal results.

B. Experimental Setup

We also developed the proposed FC-VSL scheme described in the preceding section into VGSim. Specifically, we simulate a stretch of freeway with four lanes. The length of the freeway is 600 m. The initial speeds of vehicles at the beginning of the freeway are set to $v_0 = 25$ m/s. At the end of the freeway, before the vehicles travel out of the freeway, their speeds are reduced to 20 m/s. An RSU is located at the end of the freeway. The RSU broadcasts the data points of the optimal trajectory to all vehicles in the form of an array of location–speed pairs. The transmission range of the wireless communication is set to 1000 m, and UDP and 802.11b are the transport and medium access control layer protocols adopted for the V2I communication.

At the beginning of the simulation, we randomly populate the road with vehicles at top free-flow speed at different traffic densities. After the warm-up period, during which all vehicles initially populated into the road finished traveling the entire road for at least once, we start to record the total fuel consumption for each vehicle when they travel out of the end of the road. The simulation runs for 400 s in simulation time, and the average fuel consumption is calculated at the end of the simulation.

C. VGSim-Based Experimental Results

Fig. 10 shows the average fuel consumption produced by VGSim for different densities under various traffic control schemes. The line on the bottom represents the theoretical results obtained from the optimal trajectory (24.025 ml) for the entire stretch of the road. "Optimal VSL" is the FC-VSL described in the preceding section. "Naive VSL" is a simple VSL scheme in which the speed limit is linearly decreased to the target speed with respect to location. This is a common VSL scheme applied in scenarios where the average vehicle
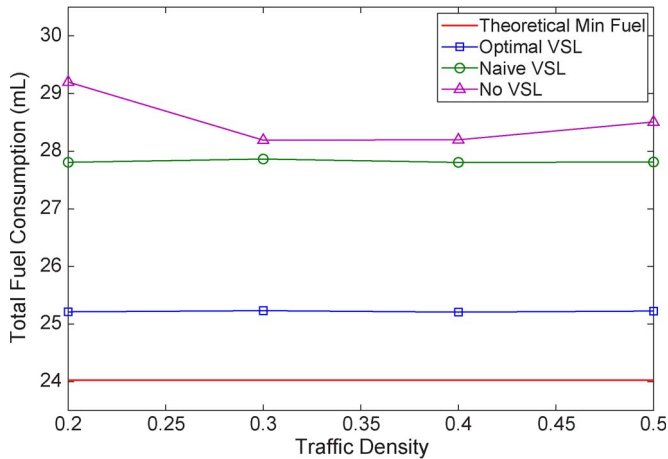
Fig. 10. Total fuel consumption under different traffic densities for different traffic control schemes.
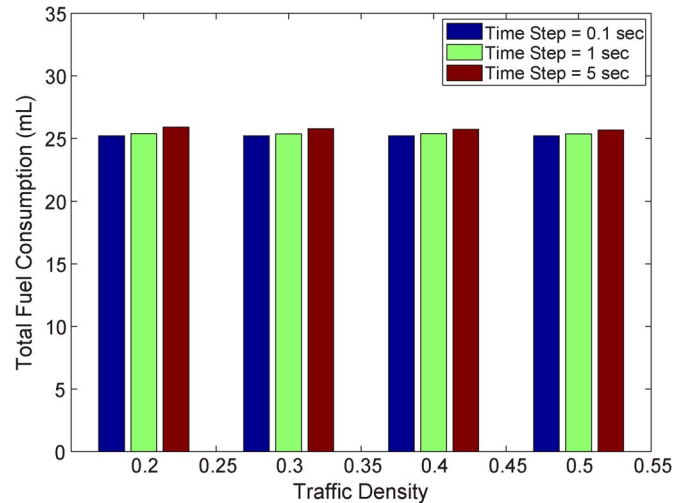

Fig. 11. Total fuel consumption under different traffic densities for different update time steps.

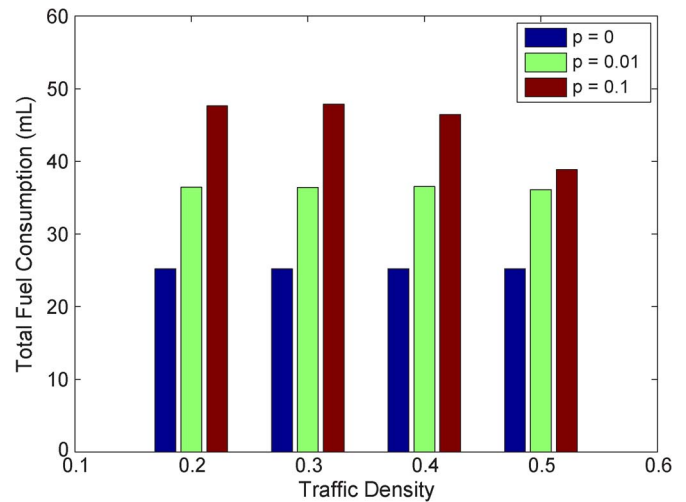Fig. 12. Total fuel consumption under different traffic densities for different slowdown probabilities (p).

speed is decreased because of traffic conditions such as drop of lane [17]. This scheme is the same as the initial guess that we provided to GOPOS. "No VSL" represents the results when no speed limit control scheme was applied. The 95% confidence interval of all data points is less than 0.1 ml and is thus not shown in the figure. For both "Optimal VSL" and "Naive VSL," the speed limit control cycle was set to 0.1 second, and the random slowdown probability at each time step was set to 0. From Fig. 10, we can see that, as previously discussed, due to the limitation of the VSL control scheme and VGSim's tendency of overestimation in the speed-reduction scenario, the "Optimal VSL" could not achieve theoretical optimal fuel consumption. However, it still results in significant reduction in the average fuel consumption, compared with "NO VSL," and outperforms the "Naive VSL" scheme. This figure also shows that density does not have significant impact on average fuel consumption. This is due to the fact, under the densities experimented, without random slowdown, most of the time, vehicles are traveling at free-flow mode under the speed limit and has minimal interaction among each other.

Since Fig. 10 shows results under the ideal environment where the control interval is at minimum and there is no random slowdown, we still need to examine the impact of control interval and random slowdown probability on the performance of the "Optimal VSL" scheme.

Fig. 11 shows the impact of a larger control interval on the "Optimal VSL"'s performance. The random slowdown probability was set to 0 in these experiments. In general, a larger control interval results in higher average fuel consumption. This is intuitive since a larger control interval will make it harder for the vehicles to follow the optimal trajectory. On the other hand, the increase in average fuel consumption is not significant if only the control interval is increased. For the largest control interval at 5 s, the distance traveled between speed limit control points could be from 90 to 125 m, which is easily implementable, even with traditional variable speed limit signs, without the need for fine-grained control infrastructures such as V2I communication.

Fig. 12 shows the random slowdown probability's impact on the total fuel consumption under the "Optimal VSL" scheme.

The control interval was set to 0.1 s. As expected, as random slowdown probability increased, the average fuel consumption dramatically increased, as the slowdown created more jitters in the traffic. At the density of 0.5, it appears that the average fuel consumption is smaller than that at other densities. This was due to the fact that, at the density of 0.5 with the high slowdown probability of 0.1, the traffic was significantly congested at the end of the road, where many vehicles travel at very low speed below the target speed of 20 m/s. The slow-downed vehicle did not suffer significantly longer travel time though, as they were already very close to the end of the road where we calculate the fuel consumption when the vehicles exit. Low speed leads to low fuel consumption at the end of the road, which, in turn, results in the reduction of the average fuel consumption. However, under real situations, the fuel consumption of the vehicles would be dramatically increased due to significant loss of speed and the increase in overall travel time.

Another important measure of any traffic control scheme is the variances of vehicle speeds at different locations across time. Small speed variances indicate smoother traffic flow, which is desirable for safety concerns. Particularly, since
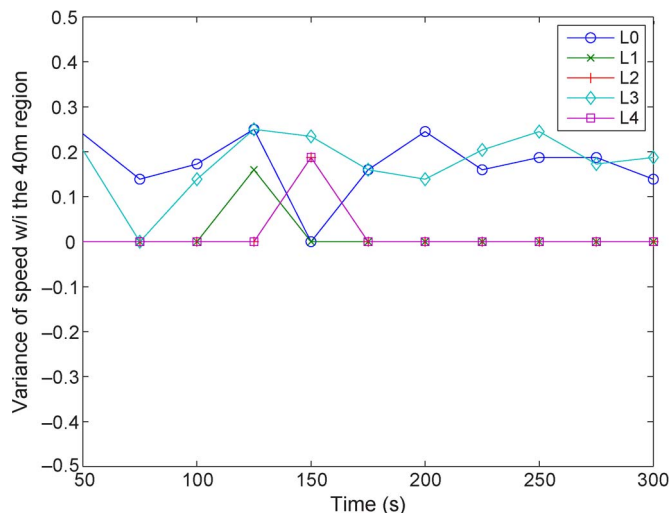
Fig. 13. Variance of speeds of vehicles at different regions across time. Traffic density $d = 0.3$ with no random slowdown ($p = 0$).

FC-VSL is not designed toward the goal of smoothing vehicular traffic, it is desirable to examine whether there is any conflict between the goal of minimizing overall fuel consumption and safety. Fig. 13 shows the variances of vehicle speeds at different regions on the road and how the variances change across time. We examine vehicles' speed variances in five regions. The starting locations of each region are given as follows: L0 and L4 are the start and end locations of the target stretch of road, respectively. L2 is the location where, according to FC-VSL, vehicles should travel at the minimum speed. L1 and L3 are in the middle between L0, L2, and L2, L4, respectively. Each region is 40 m in length. We ran the simulation with FC-VSL enabled and set the random slowdown probability of each vehicle to be zero. After the system stabilized, every 25 s, we took a snapshot of the vehicles on the road. Within each region, we calculated the variances of speeds of all vehicles in that region. Fig. 13 shows that, under FC-VSL, the speed variances in all regions are small (all smaller than 0.3 $(m/s)^2$). In addition, there was no dramatic changes of speed variances in any region across time, which means that FC-VSL do not create shockwaves that disturb traffic flow. In general, it shows that the FC-VSL scheme does not compromise safety on the road.

D. Discussion

As all of the preceding results are obtained through simulation, one potential concern would be how practical FC-VSL would be. One assumption made by FC-VSL is that, given the optimal trajectory in the form of speed limit control messages, all vehicles could follow the optimal trajectory as close as possible. This is feasible for light or medium traffic, in which vehicle interactions are rare. In case of heavy traffic or scenarios that have congestion or traffic shockwaves, vehicles may not be able to follow the advised optimal trajectory due to traffic dynamics constraints imposed by other vehicles. Therefore, in those cases, different dynamic speed control schemes targeting to reduce fuel consumption are desired. On the other hand, under light or medium traffic condition, where there are not many vehicle interactions, FC-VSL's simplicity makes it

feasible for practical use. In particular, as our result shows, even when the updating interval is long (about 5 s), the total fuel consumption is similar with very fine updating intervals. This means that, even when using traditional speed detection and control technologies such as loop detectors and VMSs, we can still achieve significant savings in fuel consumption demonstrated by FC-VSL.

VII. CONCLUSION

In this paper, we have proposed FC-VSL, which is a variable speed limit control scheme that targets to minimize average vehicular carbon footprint/fuel consumptions under certain traffic conditions. We have first derived an individual vehicle's theoretical optimal moving trajectory, which can result in minimum fuel consumption. Then, based on the optimal trajectory, we have designed the FC-VSL scheme so that all vehicles are allowed to follow the optimal trajectory as close as possible. Through simulation, it showed that FC-VSL can significantly reduce the average fuel consumption of the vehicle, achieving results close to the optimum. It also outperformed another VSL scheme designed for smoothing vehicular traffic. The system parameters' impact on the performance of FC-VSL has also been studied. Results showed that, while both high speed control interval and high driver random slow probability resulted in more fuel consumption, the latter had a much higher negative impact on the performance of FC-VSL. In addition, we also examined FC-VSL's impact on the smoothness of traffic flow. It showed that, under FC-VSL, variances of vehicle speeds were low at different regions on the road and that there were no dramatic changes of speed variance across time.

REFERENCES

[1] "U.S. Greenhouse Gas Inventory Report," U.S. Environ. Protection Agency, Washington, DC, Apr. 2011.
[2] "Climate Change 2007: The Physical Science Basis," in *Contribution of Working Group I to the Fourth Assessment Report of the Intergovernmental Panel on Climate Change. IPCC*, May 4, 2007.
[3] R. Uzcategui and G. Acosta-Marum, "WAVE: A tutorial," *IEEE Commun. Mag.*, vol. 47, no. 5, pp. 126–133, May 2009.
[4] [Online]. Available: http://www.fueleconomy.gov/feg/contentIncludes/climate_inc.htm
[5] *Greenhouse Gas Emissions*. [Online]. Available: http://epa.gov/climatechange/emissions/index.html
[6] *Carbon Footprint*. [Online]. Available: http://www.fueleconomy.gov/feg/emissions/GHGemissions.htm
[7] R. Akcelik and M. Besley, "Operating cost, fuel consumption, and emission models in aaSIDRA and aaMOTION," in *Proc. 25th Conf. Australian Inst. Transport Res. (CAITR)*, Adelaide, Australia, Dec. 3–5, 2003.
[8] "Getting the genie back in the bottle: Limiting speed to reduce carbon emissions and accelerate the shift to low carbon vehicles," in *Proc. Low-CVP*, 2005, pp. 22–32.
[9] [Online]. Available: http://safety.fhwa.dot.gov/speedmgt/vslimits/
[10] *Examples of Variable Speed Limit Applications*. [Online]. Available: http://safety.fhwa.dot.gov/speedmgt/vslimits/docs/vslexamples.ppt
[11] M. Zarean, P. Pisano, K. Dirnberger, and M. Robinson, "Variable speed limit systems: The-state-of-the-practise," in *Proc. Rural Adv. Technol. Transp. Syst. Conf.*, 1999.
[12] B. Khorashadi, B. Liu, D. Ghosal, C. N. Chuah, and M. Zhang, "Smoothing vehicular traffic flow with VGrid," in *Proc. Transp. Res. Board Annu. Meeting*, Access No. 01152220, 2010.
[13] *MOBILE 6 Vehicle Emission Modelling Software*. [Online]. Available: http://www.epa.gov/oms/m6.htm
[14] *MOVES (MOtor Vehicle Emission Simulator)*. [Online]. Available: http://www.epa.gov/otaq/models/moves/index.htm

[15] *The EMission FACtors Model*. [Online]. Available: http://www.arb.ca.gov/msei/onroad/latest_version.htm
[16] *U.K. Emission Factors Database*. [Online]. Available: http://www.naei.org.uk/other/vehicle_emissions_v8.xls
[17] P. Lin, K. Kang, and G. Chang, "Exploring the effectiveness of variable speed limit controls on highway work-zone operations," *J. Intell. Transp. Syst.*, vol. 8, no. 3, pp. 155–168, Jul. 2004.
[18] *Induction Loop*. [Online]. Available: http://en.wikipedia.org/wiki/Induction_loop
[19] F. L. Mannering, S. S. Washburn, and W. P. Kilareski, *Principles of Highway Engineering and Traffic Analysis*, 4th ed. Hoboken, NJ: Wiley, 2009.
[20] D. A. Benson, "A Gauss pseudospectral transcription for optimal control," Ph.D. dissertation, Dept. Aeronaut. Astronautics, Mass. Inst. Technol., Cambridge, MA, May, 2007.
[21] B. Liu, B. Khorashadi, H. Du, C. Chuah, M. Zhang, and D. Ghosal, "VGSim: An integrated networking and microscopic vehicular mobility simulation platform," *IEEE Commun. Mag.*, vol. 47, no. 5, pp. 134–141, May 2009.
[22] GPOPS. [Online]. Available: http://www.gpops.org/
[23] SNOPT. [Online]. Available: http://www.sbsi-sol-optimize.com/asp/sol_product_snopt.htm
[24] K. Nagel and M. Schreckenberg, "A cellular automation model for freeway traffic," *J. Phys.*, vol. 2, no. 12, pp. 2221–2229, Dec. 1992.
[25] Jist/SWANS. [Online]. Available: http://jist.ece.cornell.edu/
[26] C. Lin, H. Peng, J. W. Grizzle, and J. Kang, "Power management strategy for a parallel hybrid electric truck," *IEEE Trans. Control Syst. Technol.*, vol. 11, no. 6, pp. 839–849, Nov. 2003.
[27] S. Delprat, J. Lauber, T. M. Guerra, and J. Rimaux, "Control of a parallel hybrid powertrain: optimal control," *IEEE Trans. Veh. Technol.*, vol. 53, no. 3, pp. 872–881, May 2004.
[28] G. Marsden, M. McDonald, and M. Brackstone, "Towards an understanding of adaptive cruise control," *Transp. Res. C, Emerg. Technol.*, vol. 9, no. 1, pp. 33–51, 2001.
[29] A. Bjornberg, "Autonomous intelligent cruise control," in *Proc. IEEE Veh. Technol. Conf.*, 1994, vol. 1, pp. 429–433.
[30] C. Han, J. Sul, S. Kim, Y. Lim, and J. Lee, "Development of intelligent cruise control system," in *Proc. IEEE Fuzzy Syst. Conf.*, 1999, vol. 1, pp. 440–443.
[31] E. Hellstrm, A. Frberg, and L. Nielsen, "A real-time fuel-optimal cruise controller for heavy trucks using road topography information," presented at the SAE World Congr., Detroit, MI, 2006, Paper 2006-01-0008.
[32] K. P. Sanketh, S. Subbarao, and K. A. Jolapara, "I2V and V2V communication based VANET to optimize fuel consumption at traffic signals," in *Proc. 13th Int. IEEE Conf. ITSC*, 2010, pp. 1251–1255.
[33] C. Chuah, D. Ghosal, M. Zhang, and H. Du, "Finer-resolution cellular automata model for intervehicle communication applications," in *Proc. Transp. Res. Board 87th Annu. Meeting,* Access No. 01099329, 2007.

Bojin Liu received the B.S. degree in computing from The Hong Kong Polytechnic University, Kowloon, Hong Kong, in 2005. He received the Ph.D. degree from the Department of Computer Science, University of California, Davis, in 2011.

His research interests include vehicular ad hoc networks, wireless networks, and parallel and distributed systems, particularly the design of next-generation transportation management systems utilizing short-range wireless communication between vehicles.

Dipak Ghosal (M'07) received the B.Tech. degree in electrical engineering from the Indian Institute of Technology, Kanpur, India, in 1983, the M.S. degree in computer science and automation from Indian Institute of Science, Bangalore, India, in 1985, and the Ph.D. degree in computer science from the University of Louisiana, Lafayette, in 1988.

He is currently a Professor with the Department of Computer Science, University of California, Davis. His research interests are high-speed and wireless networks, with particular emphasis on the impact of new technologies on network- and higher layer protocols and applications, the application of parallel architectures for protocol processing in high-speed networks, and the application of distributed computing principles in the design of next-generation network architectures and server technologies.

Chen-Nee Chuah (M'01–SM'06) received the B.S.E.E. degree from Rutgers University, Camden, NJ, and the M.S. and Ph.D. degrees in electrical engineering and computer sciences from the University of California, Berkeley.

She is currently a Professor with the Department of Electrical and Computer Engineering, University of California, Davis. Her research interests include Internet measurements, network management, and wireless/mobile computing.

Dr. Chuah is an Associate Editor for the IEEE/ACM TRANSACTIONS ON NETWORKING.

H. Michael Zhang received the B.S.C.E. degree from Tongji University, Shanghai, China, and the M.S. and Ph.D. degrees in engineering from the University of California, Irvine.

He is currently a Professor with the Department of Civil and Environmental Engineering, University of California, Davis. He is an Area Editor for the *Journal of Networks and Spatial Economics* and Associate Editor for *Transportation Research—Part B: Methodological*. His research interests include transportation systems analysis and operations.